

Immunohistological analysis of B7-H4, IDO1, and PD-L1 expression and tumor immune microenvironment based on triple-negative breast cancer subtypes

Fumiaki Sanuki¹, Yuka Mikami¹, Hirotake Nishimura¹, Yoshinori Fujita¹, Yasumasa Monobe², Tsunehisa Nomura³, Naruto Taira³, and Takuya Moriya^{1,*}

¹Department of Pathology, Kawasaki Medical School, Kurashiki, Okayama, Japan

²Department of Pathology, Kawasaki Medical School General Medical Center, Okayama, Japan

³Department of Breast and Thyroid Surgery, Kawasaki Medical School, Kurashiki, Japan

***Corresponding author:** Takuya Moriya, MD

Kawasaki Medical School, Department of Pathology

577 Matsushima, Kurashiki, 701-0192, Japan

Phone: 81 86 462 1111

Fax: 81 86 462 1199

E-mail: tmoriya@med.kawasaki-m.ac.jp

ABSTRACT

Background: B7 homolog 4 (B7-H4) and indoleamine 2,3-dioxygenase (IDO1) are factors involved in the inhibition of antitumor activity and are new therapeutic targets for immune checkpoint therapy. Our study aimed to simultaneously investigate the interrelationship among B7-H4, IDO1 and programmed cell death ligand 1 (PD-L1) expression in triple-negative breast cancer (TNBC), including tumor immune microenvironment (TIME) and TNBC subtypes.

Methods: Immunostaining for PD-L1, B7-H4, and IDO1 was performed on whole-slide sections of 119 cases of TNBC. The TIME was evaluated based on stromal tumor infiltrating lymphocytes (sTILs; %), pattern classification of TILs, tumor–stroma ratio (TSR), and tertiary lymphoid structure (TLS). TNBC subtypes were also determined by immunohistochemistry analysis of cytokeratin 5/6 and androgen receptor (AR) expression.

Results: B7-H4 expression was significantly higher in cases with a combined positive score cutoff of 5 for PD-L1 (clone 28-8; $p = 0.021$), inflamed TIL pattern ($p = 0.007$), and $TLS \geq 4$ ($p = 0.006$). B7-H4 expression was higher in case of $CK5/6 \geq 10$ ($p = 0.035$). The H-scores of AR and B7-H4 were inversely correlated ($\rho = -0.509$, $p < 0.001$). B7-H4 and IDO1 expression levels were inversely correlated in cases with $AR < 10$ ($\rho = -0.354$, $p < 0.001$).

Conclusions: These results suggest that considering the TIL pattern and TLS and identifying the expression of PD-L1 and the basal-like type are useful for estimating B7-H4 expression. In addition, luminal androgen receptor (LAR)-type is frequently deficient in B7-H4 expression. In non-LAR types, B7-H4 and IDO1 expression are exclusive.

Keywords: Breast cancer; Triple-negative breast cancer; Immune checkpoint molecules; Immune checkpoint inhibitors; Tumor-infiltrating lymphocytes

INTRODUCTION

Triple-negative breast cancer (TNBC) is a hormone-receptor (estrogen receptor [ER] and progesterone receptor [PgR])- and human epidermal growth factor receptor 2 (HER2)-negative breast cancer that is often difficult to treat because of its poor prognosis and limited effective treatment options. While new treatments for breast cancer, including TNBC, have emerged in recent years, more appropriate treatment options are required [1].

Immune checkpoint inhibitor (ICI) therapy, which promotes anti-tumor immunity by targeting immune checkpoint molecules (ICMs), has revolutionized cancer treatment strategies. In November 2020, following the first clinical trial for the treatment of locally recurrent or metastatic programmed cell death ligand 1 (PD-L1)-unresectable (PD-L1 clone 22C3 combined positive score [CPS] ≥ 10) TNBC, the anti-programmed cell death (PD-1) antibody, pembrolizumab, in combination with chemotherapy received FDA approval [2]. However, the effectiveness of ICIs in breast cancer is limited, and the eventual development of treatment resistance is a challenge. Therefore, additional treatment options are required.

One promising ICM as a therapeutic target is B7 homolog 4 (B7-H4), a type I transmembrane protein belonging to the B7 family of proteins, also known as B7x, B7 super family member 1 (B7S1), and V-Set Domain Containing T Cell Activation Inhibitor 1 (VTCN1), which has shown mRNA and protein expression in serous ovarian and breast cancers [3]. Although messenger ribonucleic acid (mRNA) expression has been reported in a wide range of organs in human normal tissues, protein expression in normal tissues is relatively low or undetected [4]. Cytokines within the tumor immune microenvironment (TIME), such as interleukin (IL)-2, IL-6, IL-10, interferon (IFN)- γ , and tumor necrosis factor (TNF)- α , are also expressed in tumor cells and have been shown to induce B7-H4 expression. Activated T cells bind specifically to B7-H4 Ig, resulting in reduced inflammatory T cell responses and increased Treg function [5]. Drug development is in the preclinical stage. Cell line xenograft model mice administered a poly-adenosine diphosphate (ADP) ribose polymerase (PARP) inhibitor combined with an antibody–drug conjugate showed an overall response rate of 69%, correlating with B7-H4 levels, and a phase 1 clinical trial of a B7-H4 targeting antibody drug conjugate is ongoing (NCT05123482) [6].

Indoleamine 2,3 dioxygenase 1 (IDO1), another ICM, is a rate-limiting enzyme that metabolizes tryptophan, an essential amino acid, into kynurenine, which is expressed in a variety of solid tumors and plays an immunosuppressive role [7]. Stress caused by tryptophan depletion in the environment interferes with T-cell function and involves not only the pathway that metabolizes tryptophan into kynurenine, but also the phosphoinositide 3-kinase-Akt-mammalian target of rapamycin (PI3K-Akt-mTOR), janus kinase/signal transducers and activators of transcription (JAK-STAT), and aryl hydrocarbon receptor (AhR) pathways. Metabolites have also been proposed to induce PD-1 in T-cells [8]. Although therapeutic agents, such as epacadostat and indoximod, have

been developed and shown excellent tolerability in Tier I/II clinical studies, the Tier III trial ECHO-301/KEYNOTE-252 in melanoma did not show a superior therapeutic effect versus placebo [9]. A phase 1/2 clinical trial of an immunomodulatory vaccine (IO102-IO103) dual targeting PD-L1 and IDO1 in melanoma in combination with nivolumab showed an overall response rate (ORR) of 80% (n = 24/30) and a median progression free survival (PFS) of 26 months.

Currently, biomarkers and their interrelationships have not been fully elucidated to predict the therapeutic efficacy of PD-L1 and other ICIs as well as the expression of B7-H4 and IDO1. It has been reported that the expression of PD-L1, B7-H4, and IDO1 showed an exclusive distribution in non-small cell lung cancer [11]. An indicator associated with the therapeutic response to ICI is the tumor mutation burden (TMB), which indicates the amount of somatic gene mutations. The TMB for breast cancer is moderate, while that for TNBC is relatively high [12]. However, there are reports that ICI is not fully effective in carcinomas in which the amount of neoantigens and tumor-infiltrating CD8⁺ lymphocytes do not match, even in TMB-high tumors [13]. Stromal tumor-infiltrating lymphocytes (sTILs) are an indicator for ICI efficacy, for which a measurement method has been proposed [14]. TIL pattern phenotypes have also been proposed, classifying TIL infiltration into three phenotypes: desert, an immunologically cold pattern with few TILs; excluded, in which TILs are predominantly present in the marginal areas of the tumor but often poorly distributed inside the tumor; inflamed, in which TILs are abundant, extend to tumor cells, and are immunologically hot [15]. Tertiary lymphoid structure (TLS), a lymph follicular structure that arises in the peritumor region, is involved in immune memory and may be a predictive indicator of ICI efficacy [16]. Additional indicators include the tumor–stroma ratio (TSR), which is based on the idea that stromal components inhibit anti-tumor immune responses [17].

The molecular subtypes of TNBC may be related to the type of treatment and outcome, and a number of subtypes have been proposed for TNBCs. Lehmann et al. suggested six molecular subtypes, including two basal-like (BL1 and BL2), immunomodulatory (IM), mesenchymal (M), mesenchymal stem-like (MSL), and luminal androgen receptor (LAR) types [18]. Using laser capture microdissection, Lehmann et al. later confirmed that the IM and MSL types originate from stromal cells in the tumor region. Therefore, the subtypes were refined to four types (TNBC type-4): BL1, BL2, M, and LAR [19]. The representative surrogate markers for these molecular subtypes include androgen receptor (AR) for the LAR type, and cytokeratin 5/6 (CK5/6) and epidermal growth factor receptor for the basal-like type [20, 21]. The use of anti-androgen drugs for the treatment of LAR-type TNBC has been attempted as a new treatment based on molecular subtype [22]. Overall, identifying biomarkers specific to these subtypes will help in selecting appropriate treatments and predicting treatment outcome. Therefore, this study, for the first time, aimed to simultaneously investigate the interrelationship among B7-H4, IDO1, PD-L1, TIME and subtypes

in TNBC by focusing on whole-slide analysis (as previous studies have mainly employed tissue microarray) to identify appropriate biomarkers for selecting and predicting treatment outcome.

MATERIALS AND METHODS

Formalin-fixed paraffin-embedded (FFPE) tissue samples of the residual block of 119 resected cases of TNBC without preoperative chemotherapy after pathological diagnosis were thinly sliced and immunohistochemically analyzed for B7-H4, IDO1, PD-L1, CD8, FOXP3, CK5/6, and AR, including the expression of each marker and immune cell (details of the antibodies used are provided in Supplemental Table 1). The PD-L1 clones selected for this study were 28-8 and SP142 because of the reported correlation between the PD-L1 clone 28-8 and 22C3 scores in TNBC [23]. Two pathologists (FS, TM) were evaluators.

Immunohistochemical staining

The paraffin blocks were thinly sliced to 4 μ m, stretched, dried, and deparaffinized with xylene. Details of the primary antibodies, staining conditions such as antigen activation and incubation methods, and positive controls are listed in Supplemental Table 1. Overall, 119 PD-L1 (SP142) clones were stained using an automated immunostaining system (VENTANA BenchMark ULTRA, Roche Diagnostics, Basel, Switzerland). Antibodies other than those for PD-L1 (SP142) were stained manually. Hydrogen peroxide was used for endogenous peroxidase treatment; the secondary antibodies were stained on a Dako EnVision+ Dual Link System-HRP (Agilent, Santa Clara, California, USA) for 30 min, and 3, 3'-diaminobenzidine (DAB) was performed using a Liquid DAB+ Substrate chromogen system (Dako, Agilent, Santa Clara, California, USA) for 5 min.

Immunostaining evaluation

B7-H4 and IDO1 were evaluated according to the H-Score. The H-score is calculated between 0 and 300 according to the sum of staining intensities from 0 to 3 multiplied by the percentage of positive tumor cells. It was calculated by multiplying the sum of the three levels of staining intensity, 0 for negative staining intensity and 1 (weak), 2 (moderate), and 3 (strong) for positive staining intensity, by the percentage of tumor cells stained. Scoring was performed by an evaluator, a pathologist, using an optical microscope and visual inspection. Representative images of each staining intensity are shown in Fig. S1. PD-L1 (SP142) was evaluated based on the number of immune cells (IC) in the tumor area according to the determination guidelines [24]. The scores for PD-L1 (28-8) were calculated by dividing the number of tumor and inflammatory cells, such as lymphocytes and macrophages, that tested positive by the total number of tumor cells and multiplying it by 100. The formula is shown in equation 1.

$$CPS = \frac{PD-L1 \text{ positive cells (tumor cells and mononuclear inflammatory cells)}}{\text{total number of tumor cells}} * 100 \quad (1)$$

While cytoplasmic positivity was sometimes detected, membrane staining was defined as positivity in tumor cells. For TNBC subclassification, immunostaining was performed for CK 5/6

and AR, with an H-score and a positive nuclear percentage of >10% as cutoffs for AR [25]. The CK 5/6 cutoffs were 1% and 10%, respectively [21, 26].

TIME evaluation

TIL% was evaluated as proposed by the TIL Working Group [14]. TIL patterns were classified into three categories: desert, excluded, and inflamed. The TLS was evaluated by counting on slides within a 5-mm area around the tumor sections [27]. TSR was calculated as the percentage of stroma in the tumor area, excluding degenerated areas [17].

Study approval

This study was conducted after obtaining approval following a review based on the ethical guidelines of the Ethics Committee of Kawasaki Medical School in accordance with the Declaration of Helsinki (approval number 5013-03). Although this was a retrospective study, each patient provided informed consent for study inclusion before surgery. A summary of the study protocol was published on a web page, which explained the study and provided an opportunity for dissenting opinions to be expressed.

Statistical analysis

IBM SPSS Statistics for Windows, version 29.0 (IBM Corp., Armonk, NY, USA) was used to perform statistical analyses. χ -square and Fisher's exact tests were used to evaluate the statistics in cross tables. The non-parametric Mann–Whitney U and Kruskal–Wallis tests were used to evaluate categorical variables, while Spearman's rank correlation coefficients were used to assess continuous variables. Prognostic statistics were assessed using the Kaplan–Meier method and log-rank tests. Statistical significance was set at $p < 0.05$.

RESULTS

Patient characteristics

The relationship between clinical pathology data and ICM expression is shown in Table 1. The patient ages ranged from 25 to 89 years, with a mean age of 60.8 years. The average invasion size was 21.3 mm, and 35 cases had lymph node metastasis. Stage I was the most common stage (57 cases, 47.9%), followed by Stage II (43 cases, 36.1%), Stage III (17 cases, 14.3%), and Stage IV (2 cases, 0.017%). The histological types included invasive ductal carcinoma (no special type) (NST, 103 cases), invasive lobular carcinoma (ILC, 1 case), adenoid cystic carcinoma (ACC, three cases), and metaplastic carcinoma (MC, four cases). Histological classification of metaplastic carcinoma included one case of matrix-producing carcinoma and three cases of spindle cell carcinoma. Overall, 86 cases received postoperative chemotherapy, radiotherapy, or both. One case was treated with ICI (atezolizumab) + nanoparticle albumin-bound paclitaxel (nab-PTX) and was classified as progressive disease.

Immunohistochemistry

Representative immunostaining findings are shown in Fig. 1; the three staining levels are shown in Fig. S1. B7-H4 stained the cytoplasmic membrane and cytoplasm of carcinoma cells. IDO1 was strongly expressed in cancer cells (positivity rate) and independently (59/119; 49.6%) in the tumor vascular endothelium (Fig. S2). CPS ≥ 1 was observed in 49 of the 119 cases (41.1%), CPS ≥ 10 in 18 (15.1%) cases, and PD-L1 (SP142) IC ≥ 1 in 71 (59.7%) cases. AR had a maximum H-score of 260, with a mean of 41.4, and 79 cases were completely negative. Three adenoid cystic carcinomas (ACC) showed CK5/6 positivity; however, because ACC differs from the molecular expression of the basal-like type, we analyzed 116 cases, excluding ACC. Among these 116 cases, 41 (35.3%) had CK 5/6 ≥ 10 and 49 (42.2%) had CK 5/6 < 1 .

Association of clinicopathological features with immune checkpoint markers

The median H-scores of B7-H4 and IDO1 were 120 and 1, respectively. The cutoffs for the CPS of PD-L1 (28-8) and the IC of PD-L1 (SP142) were both 1 (Table 1). B7-H4 expression was significantly low in patients aged >55 years. A high histological grade was significantly associated with high expression levels of B7-H4, PD-L1 (28-8), and PD-L1 (SP142) ($p = 0.023$, 0.002 , and 0.003 , respectively). A total of eight cases were apocrine carcinoma, all of which were negative for B7-H4. B7-H4 expression differed significantly only for CK 5/6, with high B7-H4 positivity in CK5/6 ≥ 10 ($p = 0.019$).

The relationship between TIME and ICM expression is shown in Table 2. The median cutoffs were used for CD8, FOXP3, TLS, and TSR. Two PD-L1 types were strongly associated with TILs and TIL patterns, but sTILs (%) < 20 and desert-pattern cases also included cases with high B7-H4

and IDO1 expression. PD-L1 (28-8) negativity was predominant in cases with a high stromal fraction (high TSR; $p = 0.001$).

All eight cases with histological findings of apocrine carcinoma showed low B7-H4 expression, (Table 1), which was also confirmed by the heatmap in Fig. 2. Although there were some exceptions, B7-H4 expression tended to be low in the cases with high AR expression.

B7-H4 expression was significantly higher in cases with inflamed TIL pattern ($p = 0.007$), TLS ≥ 4 ($p = 0.006$), and higher numbers of peritumoral CD8-positive T-cells ($p = 0.014$; Fig. 3a), while AR expression was significantly higher in cases showing a desert TIL pattern ($p = 0.045$; Fig. 3b). AR expression was also significantly higher in the group with TLS < 4 ($p = 0.044$). AR expression was significantly lower in cases with high numbers of peritumoral CD8-positive T-cells ($p = 0.014$). PD-L1 (28-8) and B7-H4 expression were both significantly lower in cases with AR ≥ 10 ($p = 0.0177$, $p < 0.001$; Fig. 3c). AR expression was significantly higher in cases with IDO1 < 1 ($p = 0.046$). B7-H4 expression was significantly higher and AR expression was significantly lower in cases with CK 5/6 ≥ 10 ($p = 0.035$ and $p < 0.001$, respectively; Fig. 3d, e).

The analysis of continuous variables between ICMs showed homology between PD-L1 (28-8) CPS and PD-L1 (SP142) IC ($p < 0.001$; Fig. 4a). The homology between PD-L1 (28-8) and B7-H4 was significantly higher in cases with PD-L1 (28-8) CPS ≥ 5 ($p = 0.021$).

Analysis of Spearman's rank correlation coefficients

We observed significant inverse correlations for AR and B7-H4 ($\rho = -0.509$, $p < 0.001$), CD8+T-cells ($\rho = -0.208$, $p = 0.023$), FOXP3+T-cells ($\rho = -0.243$, $p = 0.008$; Fig. 4b), and Ki-67 labeling index ($\rho = -0.521$, $p < 0.001$). In the overall population, B7-H4 and IDO1 were not significantly correlated ($\rho = -0.054$, $p = 0.558$), while B7-H4 and PD-L1 (SP142) were positively correlated ($\rho = 0.245$, $p = 0.019$; Fig. 5a). In the subgroup analysis of AR < 10 to validate the expression of ICMs and TIME status of subtypes other than LAR, B7-H4 and IDO were negatively correlated ($\rho = -0.354$, $p < 0.001$; Fig. 5b).

Prognosis

Overall survival (OS) was better in the PD-L1 (28-8) CPS ≥ 10 group than in the PD-L1 (28-8) group with CPS greater than 0 but less than 1. The OS was also significantly better in cases with TSR < 45 (Fig. S3). PFS was significantly better in cases with high IDO1 expression ($p = 0.038$; Fig. S4). AR showed no significant differences in OS and PFS. The CK5/6 ≥ 10 group had a significantly worse PFS than the CK5/6 < 1 group ($p = 0.008$). Spearman's rank correlation coefficients showed that AR and age were directly proportional ($\rho = 0.317$, $p < 0.001$). The results of the Mann-Whitney U test showed that cases with CK 5/6 < 10 were significantly younger ($p = 0.036$).

DISCUSSION

The results of this study showed that cases with high B7-H4 expression had a relatively young age, high Ki-67 labeling index and histological grade, were of the basal-like (BL) type, and not the LAR type. These cases exhibited an inflamed TIL pattern, and the number of peritumoral CD8+ T-cells, FOXP3+ T-cells, and TLS was high. B7-H4 expression is considered to increase regulatory T-cell and decrease cytotoxic T-cell counts [4, 5]. Nevertheless, there are two possible reasons for the highly immunogenic characteristics. One possibility is that in cases that show an inflamed TIL pattern, upregulation of B7-H4 expression by inflammatory cytokines may be occurring as well. Another possible cause is that results were obtained from indirect comparisons between different immunogenic subtypes. Differences in immunogenicity between BL and LAR types and their association with B7-H4 may hinder a proper assessment of the relationship between TIME and B7-H4.

IDO1 was expressed in tumors characterized by high sTILs (%) and inflamed or excluded TIL patterns at a cutoff of 1%. However, we may have observed upregulation of IDO1 due to concurrent inflammation. In this study, IDO1 was stained in the vascular endothelium in the tumor region and TLS, including cases in which there was no IDO1 expression in the tumor. We classified IDO1 staining intensity of the vascular endothelium in the tumor region into three levels and examined its relationship with the TIME, which was significantly proportional to sTILs (%) and CD8+, FOXP3+ T-cells in the tumor region (Fig. S2). Evaluation of IDO may be important not only in tumor tissue but also in background tissue.

In relation to PD-L1, PD-L1 (28-8) showed high B7-H4 expression in cases with CPS ≥ 5 . Moreover, PD-L1(SP142) IC and B7-H4 H-scores showed a significant positive correlation. This contradicts a report that PD-L1 and B7-H4 were exclusive in various intrinsic subtypes of breast cancer, including TNBC [28]. This report used tissue microarray and evaluated PD-L1 in tumors and stroma by quantitative immunofluorescence using SP142, which differs from the method used in our study. The PD-L1 (28-8) CPS ≥ 10 group tended to have higher expression of IDO1, although not significant. Noura et al. reported a correlation between PD-L1 and IDO1 expression in breast cancer and a relationship with highTILs in TNBC [29], which is partially consistent with our findings.

In the examination of molecular subtypes, AR expression was almost absent in cases with CK5/6 ≥ 10 , possibly indicating differences in molecular subtypes. The expression of AR was inversely correlated with the expression level of B7-H4 in our study. The scatter plots showing the relationship between B7-H4 and AR in Fig. 4b indicates that few cases expressed both B7-H4 and AR, and that mostly one or the other was expressed. Wang et al. reported an inverse correlation between AR and B7-H4 in immunohistochemistry of TNBC [30].

Whether this finding was due to differences in tumor characteristics or whether AR prevents the expression of B7-H4 is unclear. IDO1 showed a significant difference between AR expression at a cutoff of 1%.

Previous reports have shown that IDO1 positivity is more common in the BL type than in LAR or claudin-low (CL) types [31]. We also observed that the BL type showed significantly higher B7-H4 expression. Kim et al. reported significantly higher tumor B7-H4 mRNA expression in the BL type as compared to an unclassifiable type of disease ($p < 0.05$) [32]. Our results are partially consistent with these previous reports. In our study, the LAR type tended to be found in patients of older age who were immunologically cold, with low histological grade, and inversely correlated with Ki-67, consistent with previous reports [20, 25]. Furthermore, the cases of this subtype tended to have low levels of PD-L1 (28-8). These results are in contrast to the characteristics of B7-H4, and may help predict the LAR type. These LAR-type characteristics may hinder an accurate evaluation of the TIME index of B7-H4 and ICM expression in the overall TNBC population.

In subgroup analysis, B7-H4 and IDO1 were significantly inversely correlated in non-LAR types, suggesting that cases without AR or B7-H4 may express IDO1. Kurt et al. reported that IFN- γ increased PD-L1 and IDO1 but not B7-H4 in lung non-small cell carcinoma cultures, while treatment with IL-10 increased B7-H4 but not PD-L1 or IDO [11]; thus, the type and priority of proinflammatory cytokines may be relevant.

We observed no correlation between PD-L1 (SP142) and B7-H4 in the non-LAR type during subgroup analysis. Moreover, no significant proportional relationship was found between B7-H4 and peritumoral CD8⁺ and FOXP3⁺ T cells in the non-LAR type. These results differ from the finding that these were proportional in the overall TNBC population. The reason for this may be that LAR and other types of TNBC have very different immunogenicity, and analysis in the overall population indirectly compares differences in subtypes, making them appear proportional.

In prognostic analysis, IDO1 and PD-L1 (28-8) expression was associated with a good prognosis. The OS and PFS were better in patients with an inflamed TIL pattern, and the group with a good prognosis tended to be more immunogenic. PD-L1 expression in metastatic TNBC appears to serve as an indicator of a good outcome following ICI therapy [33]. However, since PD-L1 expression is essentially strongly dependent on the TIME, it is important to investigate how to control tumors with cold TIL patterns. B7-H4 and IDO1 expression has also been detected in some cases with a desert TIL pattern; however, it should be noted that the desert TIL pattern of TNBC is more likely to be of the LAR type and ICM expression may be insufficient.

Clinical trials of a B7-H4-targeting antibody–drug conjugate are ongoing [6], and this study suggests that drugs targeting B7-H4 may not be suitable for the LAR type. However, in TNBC, anti-androgen drugs are a promising new option [22]. Moreover, even if the non-LAR type is B7-H4 negative, it is expected to be IDO1 positive. The relationship between ICM expression, molecular

subtypes, and the TIME shown in this study may help to determine which cases are indicated for future TNBC therapy.

Our study has several limitations. First, with respect to PD-L1 clones, this study stained for PD-L1 (28-8), which may differ from the PD-L1 (22C3) score. Second, only 12 cases showed 1% B7-H4 expression in our study, which was not sufficient for comparison with the negative group. The TIME assessment showed that the lymphocyte distribution was a mixture of dense and sparse areas; thus, cell counting at four sites with many CD8⁺ and FOXP3⁺ cells may overestimate the lymphocytic infiltration of the tumor. As CD8⁺ cells include cells other than cytotoxic T-cells, T-cell exhaustion could not be assessed. Third, it is important to perform formalin fixation immediately after surgery and fixation should not go beyond 72 h. Herein, we could ensure this for relatively recent cases, but could not guarantee the same for cases older than 10 years.

This study was based on an observational design. In addition, part of the methodology involved subjective evaluation. Further objective and specific studies to substantiate the results obtained in this study are desirable.

Acknowledgments

We thank Mrs. Kaoru Tsuboi, Mrs. Megumi Kuriyama, and Mr. Nobuhisa Iwachidou for their technical assistance.

COMPLIANCE WITH ETHICAL STANDARDS

Conflict of Interest

The authors declare no conflict of interest.

Funding

This work was supported by JSPS KAKENHI (Grant number 21K06934) and Research Project Grants from Kawasaki Medical School (R04G002).

Ethical Approval

This study was conducted after obtaining approval from the Ethics Committee of Kawasaki Medical School and in accordance with the Declaration of Helsinki (approval number 5013-03).

Informed Consent

Although this was a retrospective study, each patient provided informed consent for study inclusion before surgery. A summary of the study protocol was published on a web page, which explained the study and provided an opportunity for dissenting opinions to be expressed.

Author Contributions

This study was designed and conceived by FS and TM. The material was prepared by Yuka-M, YF, and FS. Data collection and statistical analysis were performed by FS. The stained specimens were evaluated by FS and TM. Technical input was provided by NH, Yuka-M, and Yasumasa-M; Clinical information was obtained by NN and NT. The first draft of the manuscript was written by FS.

REFERENCES

1. Iacopetta D, Ceramella J, Baldino N, Sinicropi MS, Catalano A. Targeting breast cancer: An overlook on current strategies. *Int J Mol Sci* 2023;24.
<https://doi.org/10.3390/ijms24043643>
2. Cortes J, Cescon DW, Rugo HS, Nowecki Z, Im SA, Yusof MM, et al. Pembrolizumab plus chemotherapy versus placebo plus chemotherapy for previously untreated locally recurrent inoperable or metastatic triple-negative breast cancer (KEYNOTE-355): A randomised, placebo-controlled, double-blind, phase 3 clinical trial. *Lancet* 2020;396:1817–28.
[https://doi.org/10.1016/S0140-6736\(20\)32531-9](https://doi.org/10.1016/S0140-6736(20)32531-9)
3. Salceda S, Tang T, Kmet M, Munteanu A, Ghosh M, Macina R, et al. The immunomodulatory protein B7-H4 is overexpressed in breast and ovarian cancers and promotes epithelial cell transformation. *Exp Cell Res* 2005;306:128–41.
<https://doi.org/10.1016/j.yexcr.2005.01.018>
4. Sica GL, Choi IH, Zhu G, Tamada K, Wang SD, Tamura H, et al. B7-H4, a molecule of the B7 family, negatively regulates T cell immunity. *Immunity* 2003;18:849–61.
[https://doi.org/10.1016/s1074-7613\(03\)00152-3](https://doi.org/10.1016/s1074-7613(03)00152-3)
5. Podojil JR, Miller SD. Potential targeting of B7-H4 for the treatment of cancer. *Immunol Rev* 2017;276:40–51. <https://doi.org/10.1111/imr.12530>
6. Kinneer K, Wortmann P, Cooper ZA, Dickinson NJ, Masterson L, Cailleau T, et al. Design and preclinical evaluation of a novel B7-H4-directed antibody-drug conjugate, AZD8205, alone and in combination with the PARP1-selective inhibitor AZD5305. *Clin Cancer Res* 2023;29:1086–101. <https://doi.org/10.1158/1078-0432.CCR-22-2630>
7. Prendergast GC, Malachowski WJ, Mondal A, Scherle P, Muller AJ. Indoleamine 2,3-dioxygenase and its therapeutic inhibition in cancer. *Int Rev Cell Mol Biol* 2018;336:175–203. <https://doi.org/10.1016/bs.ircmb.2017.07.004>
8. Fujiwara Y, Kato S, Nesline MK, Conroy JM, DePietro P, Pabla S, et al. Indoleamine 2,3-dioxygenase (IDO) inhibitors and cancer immunotherapy. *Cancer Treat Rev* 2022;110:102461. <https://doi.org/10.1016/j.ctrv.2022.102461>
9. Long GV, Dummer R, Hamid O, Gajewski TF, Caglevic C, Dalle S, et al. Epcadostat plus pembrolizumab versus placebo plus pembrolizumab in patients with unresectable or metastatic melanoma (ECHO-301/KEYNOTE-252): A phase 3, randomised, double-blind study. *Lancet Oncol* 2019;20:1083–97. [https://doi.org/10.1016/S1470-2045\(19\)30274-8](https://doi.org/10.1016/S1470-2045(19)30274-8)
10. Kjeldsen JW, Lorentzen CL, Martinenaite E, Ellebaek E, Donia M, Holmstroem RB, et al. A phase 1/2 trial of an immune-modulatory vaccine against IDO/PD-L1 in combination with nivolumab in metastatic melanoma. *Nat Med* 2021;27:2212–23.
<https://doi.org/10.1038/s41591-021-01544-x>

11. Schalper KA, Carvajal-Hausdorf D, McLaughlin J, Altan M, Velcheti V, Gaule P, et al. Differential expression and significance of PD-L1, IDO-1, and B7-H4 in human lung cancer. *Clin Cancer Res* 2017;23:370–8. <https://doi.org/10.1158/1078-0432.CCR-16-0150>
12. O'Meara TA, Tolaney SM. Tumor mutational burden as a predictor of immunotherapy response in breast cancer. *Oncotarget* 2021;12:394–400. <https://doi.org/10.18632/oncotarget.27877>
13. McGrail DJ, Pilié PG, Rashid NU, Voorwerk L, Slagter M, Kok M, et al. High tumor mutation burden fails to predict immune checkpoint blockade response across all cancer types. *Ann Oncol* 2021;32:661–72. <https://doi.org/10.1016/j.annonc.2021.02.006>
14. El Bairi K, Haynes HR, Blackley E, Fineberg S, Shear J, Turner S, et al. The tale of TILs in breast cancer: A report from the International Immuno-Oncology Biomarker Working Group. *NPJ Breast Cancer* 2021;7:150. <https://doi.org/10.1038/s41523-021-00346-1>
15. Liu YT, Sun ZJ. Turning cold tumors into hot tumors by improving T-cell infiltration. *Theranostics* 2021;11:5365–86. <https://doi.org/10.7150/thno.58390>
16. Vaghjiani RG, Skitzki JJ. Tertiary lymphoid structures as mediators of immunotherapy response. *Cancers (Basel)* 2022;14. <https://doi.org/10.3390/cancers14153748>
17. Hagenaaars SC, Vangangelt KMH, Van Pelt GW, Karancsi Z, Tollenaar RAEM, Green AR, et al. Standardization of the tumor-stroma ratio scoring method for breast cancer research. *Breast Cancer Res Treat* 2022;193:545–53. <https://doi.org/10.1007/s10549-022-06587-3>
18. Lehmann BD, Bauer JA, Chen X, Sanders ME, Chakravarthy AB, Shyr Y, et al. Identification of human triple-negative breast cancer subtypes and preclinical models for selection of targeted therapies. *J Clin Invest* 2011;121:2750–67. <https://doi.org/10.1172/JCI45014>
19. Lehmann BD, Jovanović B, Chen X, Estrada MV, Johnson KN, Shyr Y, et al. Refinement of triple-negative breast cancer molecular subtypes: Implications for neoadjuvant chemotherapy selection. *PLoS One* 2016;11:e0157368. <https://doi.org/10.1371/journal.pone.0157368>
20. Kumar S, Bal A, Das A, Bhattacharyya S, Laroia I, Khare S, et al. Molecular subtyping of triple negative breast cancer by surrogate immunohistochemistry markers. *Appl Immunohistochem Mol Morphol* 2021;29:251–7. <https://doi.org/10.1097/PAI.0000000000000897>
21. Kim S, Moon BI, Lim W, Park S, Cho MS, Sung SH. Feasibility of classification of triple negative breast cancer by immunohistochemical surrogate markers. *Clin Breast Cancer* 2018;18:e1123–32-e32. <https://doi.org/10.1016/j.clbc.2018.03.012>
22. Choupani E, Mahmoudi Gomari M, Zanganeh S, Nasser S, Haji-Allahverdipoor K, Rostami N, et al. Newly developed targeted therapies against the androgen receptor in triple-negative breast cancer: A review. *Pharmacol Rev* 2023;75:309–27. <https://doi.org/10.1124/pharmrev.122.000665>

23. Huang X, Ding Q, Guo H, Gong Y, Zhao J, Zhao M, et al. Comparison of three FDA-approved diagnostic immunohistochemistry assays of PD-L1 in triple-negative breast carcinoma. *Hum Pathol* 2021;108:42–50. <https://doi.org/10.1016/j.humpath.2020.11.004>
24. Vennapusa B, Baker B, Kowanetz M, Boone J, Menzl I, Bruey JM, et al. Development of a PD-L1 complementary diagnostic immunohistochemistry assay (SP142) for atezolizumab. *Appl Immunohistochem Mol Morphol* 2019;27:92–100. <https://doi.org/10.1097/PAI.0000000000000594>
25. Vtorushin S, Dulesova A, Krakhmal N. Luminal androgen receptor (LAR) subtype of triple-negative breast cancer: Molecular, morphological, and clinical features. *J Zhejiang Univ Sci B* 2022;23:617–24. <https://doi.org/10.1631/jzus.B2200113>
26. Hashmi AA, Naz S, Hashmi SK, Hussain ZF, Irfan M, Bakar SMA, et al. Cytokeratin 5/6 and cytokeratin 8/18 expression in triple negative breast cancers: Clinicopathologic significance in South-Asian population. *BMC Res Notes* 2018;11:372. <https://doi.org/10.1186/s13104-018-3477-4>
27. Sofopoulos M, Fortis SP, Vaxevanis CK, Sotiriadou NN, Arnogiannaki N, Ardavanis A, et al. The prognostic significance of peritumoral tertiary lymphoid structures in breast cancer. *Cancer Immunol Immunother* 2019;68:1733–45. <https://doi.org/10.1007/s00262-019-02407-8>
28. Altan M, Kidwell KM, Pelekanou V, Carvajal-Hausdorf DE, Schalper KA, Toki MI, et al. Association of B7-H4, PD-L1, and tumor infiltrating lymphocytes with outcomes in breast cancer. *NPJ Breast Cancer* 2018;4:40. <https://doi.org/10.1038/s41523-018-0095-1>
29. Alkhayyal N, Elemam NM, Hussein A, Magdub S, Jundi M, Maghazachi AA, et al. Expression of immune checkpoints (PD-L1 and IDO) and tumour-infiltrating lymphocytes in breast cancer. *Heliyon* 2022;8:e10482. <https://doi.org/10.1016/j.heliyon.2022.e10482>
30. Wang L, Yang C, Liu XB, Wang L, Kang FB. B7-H4 overexpression contributes to poor prognosis and drug-resistance in triple-negative breast cancer. *Cancer Cell Int* 2018;18:100. <https://doi.org/10.1186/s12935-018-0597-9>
31. Kim S, Park S, Cho MS, Lim W, Moon BI, Sung SH. Strong correlation of indoleamine 2,3-dioxygenase 1 expression with basal-like phenotype and increased lymphocytic infiltration in triple-negative breast cancer. *J Cancer* 2017;8:124–30. <https://doi.org/10.7150/jca.17437>
32. Kim NI, Park MH, Cho N, Lee JS. Comparison of the clinicopathologic features and T-cell infiltration of B7-H3 and B7-H4 expression in triple-negative breast cancer subtypes. *Appl Immunohistochem Mol Morphol* 2022;30:246–56. <https://doi.org/10.1097/PAI.0000000000001001>

33. Khan M, Du K, Ai M, Wang B, Lin J, Ren A, et al. PD-L1 expression as biomarker of efficacy of PD-1/PD-L1 checkpoint inhibitors in metastatic triple negative breast cancer: A systematic review and meta-analysis. *Front Immunol* 2023;14:1060308. <https://doi.org/10.3389/fimmu.2023.1060308>

FIGURE LEGENDS

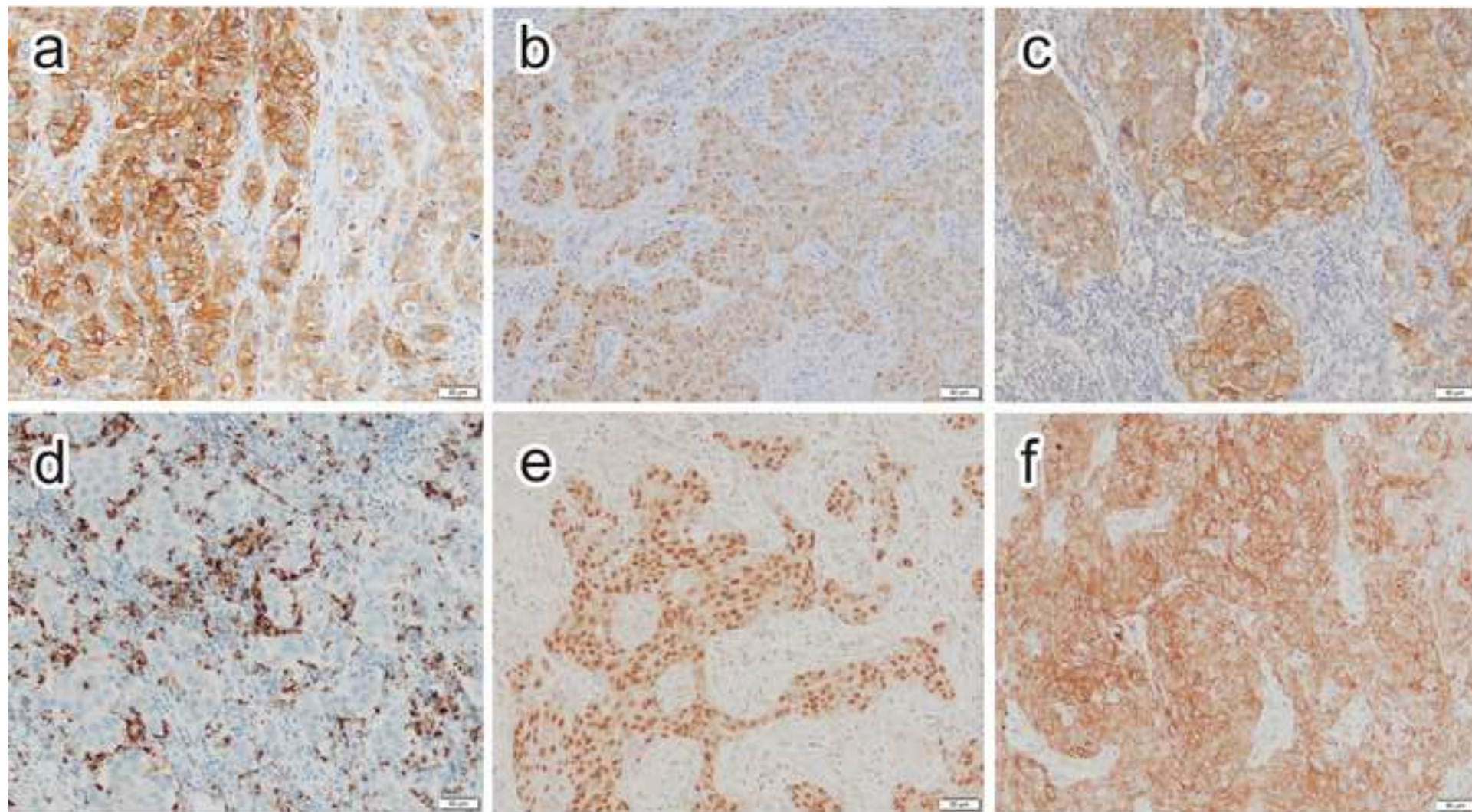
Fig. 1 Representative examples of immunohistochemical staining for triple-negative breast cancer. a B7-H4; b IDO1; c PD-L1 (clone 28-8); d PD-L1 (clone SP142); e androgen receptor (AR); f cytokeratin (CK) 5/6

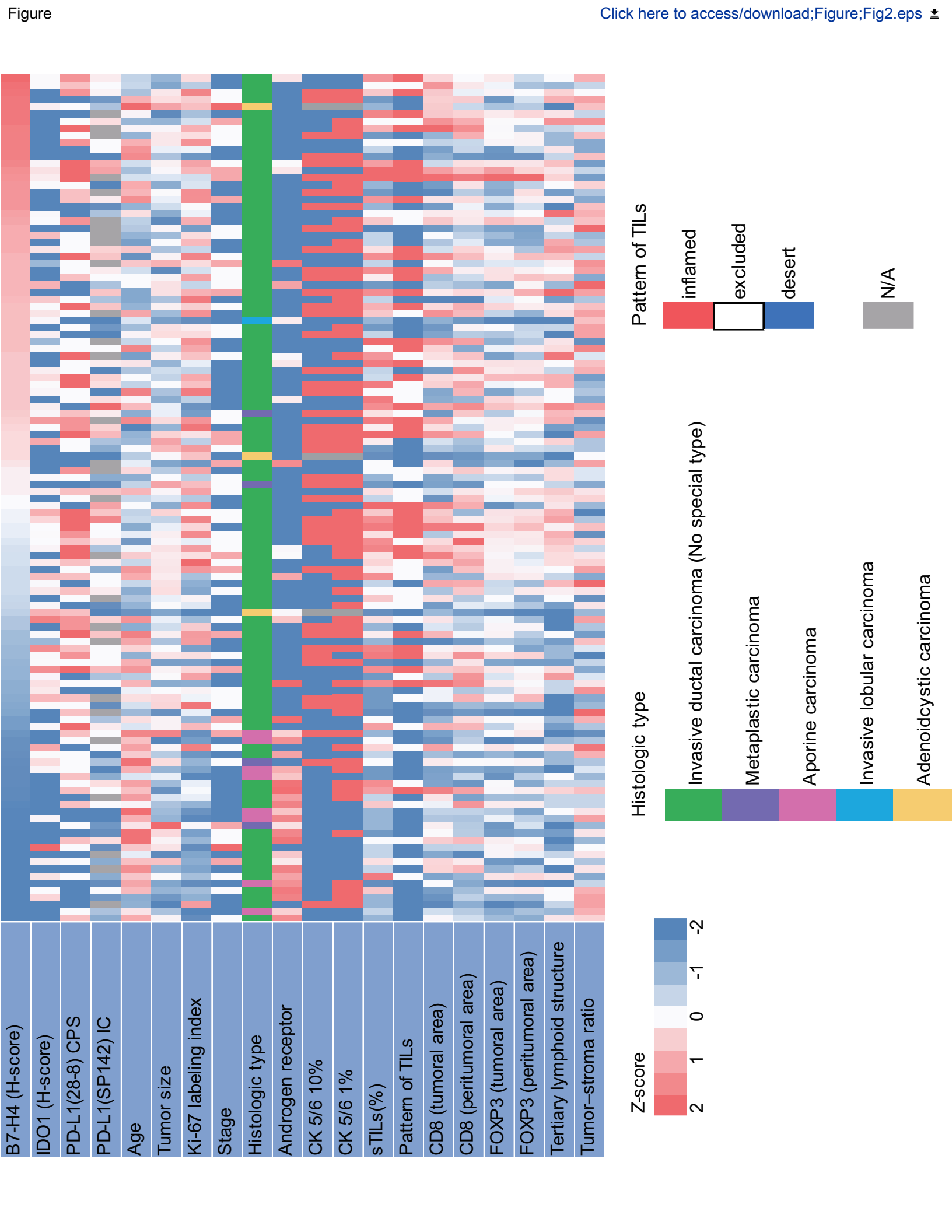
Fig. 2 Heatmap of immune checkpoint molecules (ICM expression vs. clinicopathological parameters and the tumor immune microenvironment (TIME)). Data on ICM expression and the TIME of 119 TNBC cases were compared using standardized scores (Z-scores). The related formula is $Z\text{-score} = (\text{value} - \text{mean}) / \text{standard deviation}$. The abscissa axis aligns each case in B7-H4 H-score order, while the ordinate axis represents each variable in the same case

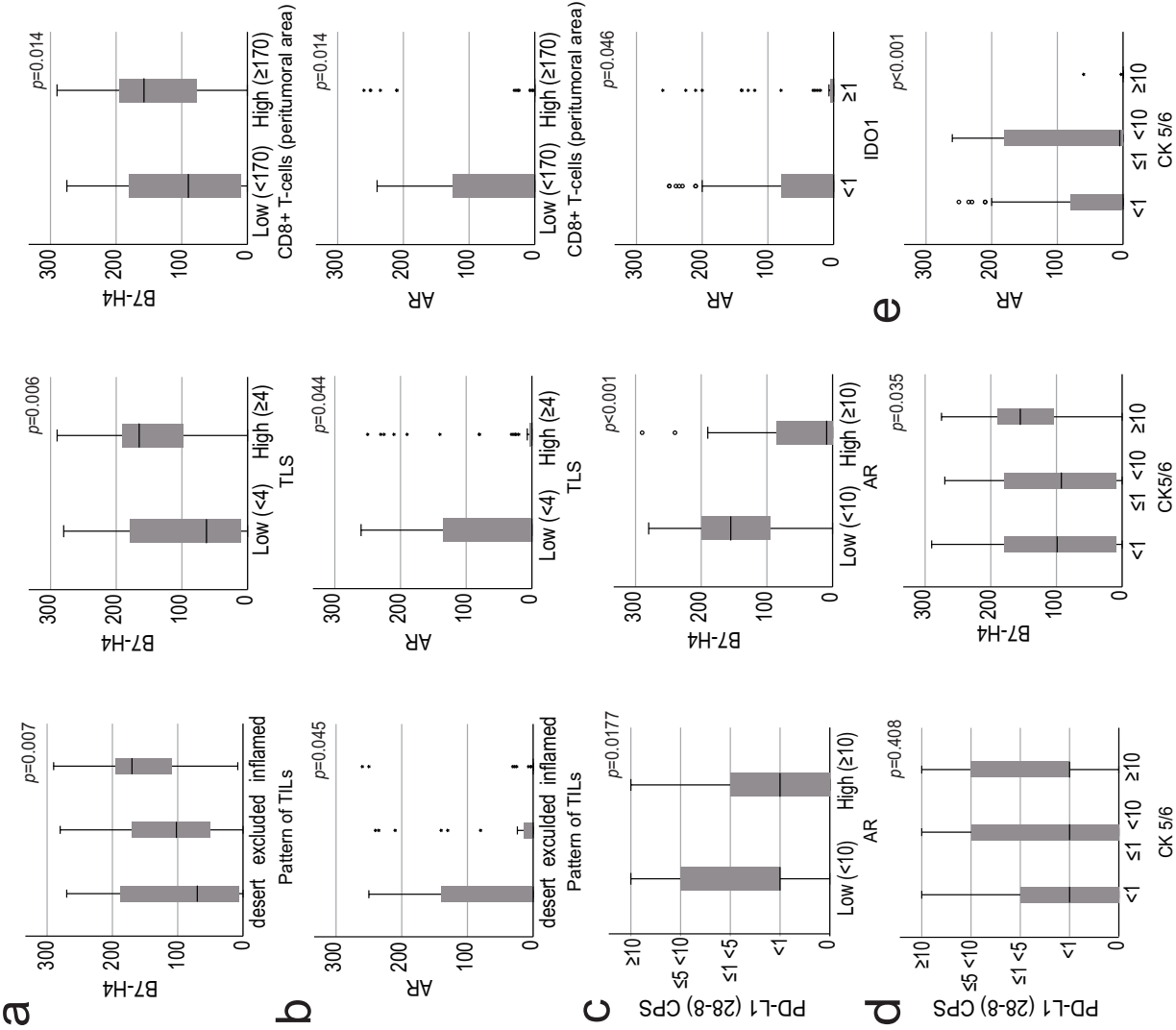
Fig. 3 Analysis of continuous variables according to subtype classification. a. Analysis of B7-H4 the H-score and tumor immune microenvironment (TIME). b. Analysis of the androgen receptor (AR) H-score and TIME. c. Analysis of AR and immune checkpoint molecule (ICM) expression. d. Analysis of cytokeratin (CK) 5/6 and ICM expression. e. Analysis of AR and CK5/6

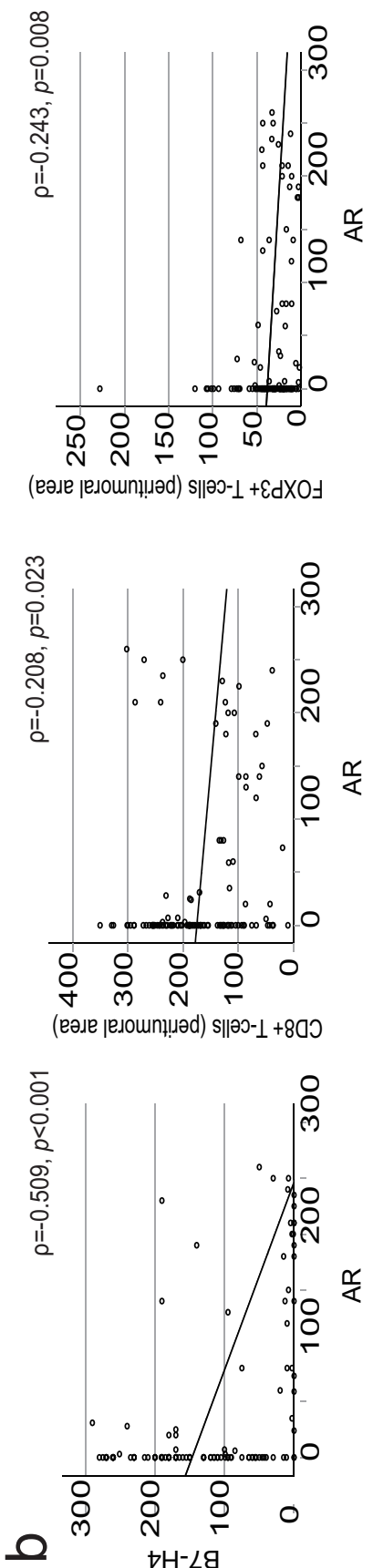
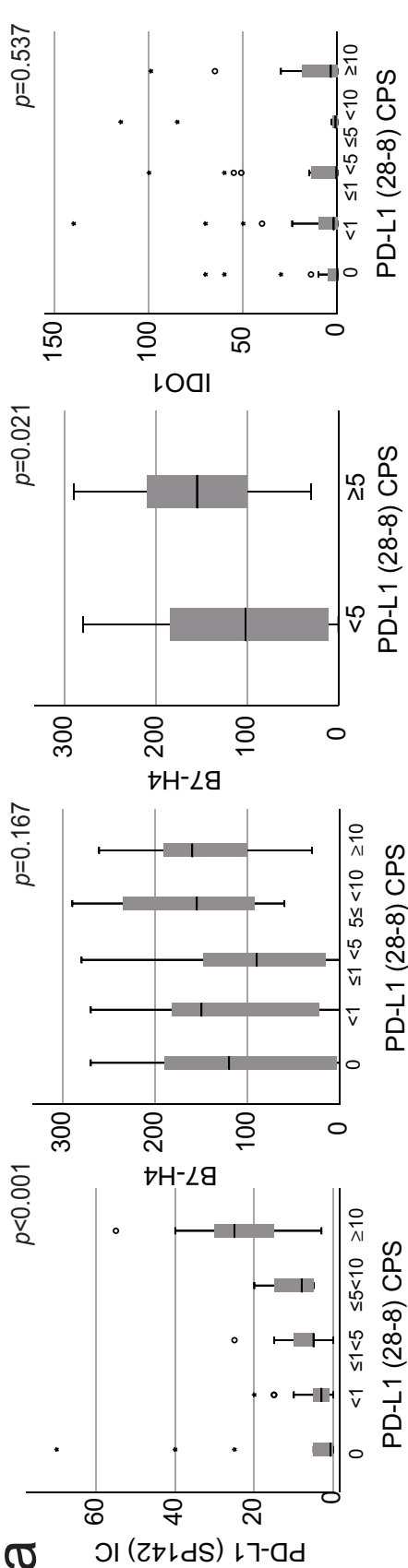
Fig. 4 Analysis of the association between immune checkpoint molecules (ICMs) and androgen receptor (AR) expression. a. Relationship between PD-L1(28-8) CPS and PD-L1 (SP142) IC and analysis of the relation between PD-L1(28-8) and B7-H4 and PD-L1(28-8) and IDO1. b. Analysis of the correlation between AR and B7-H4, AR, and CD8+, and AR and FOXP3+T-cells

Fig. 5 Comparison of ICM expression and TIME relationships between the overall population and non-LAR types a. Correlations between B7-H4 and PD-L1 and B7-H4 and IDO1 and B7-H4 in the overall population and relationship between CD8+ and FOXP3+T-cells. b. Correlations between B7-H4 and PD-L1 and B7-H4 and those between IDO1 and CD8+ and IDO1 FOXP3 +T-cells in cases with low AR expression.

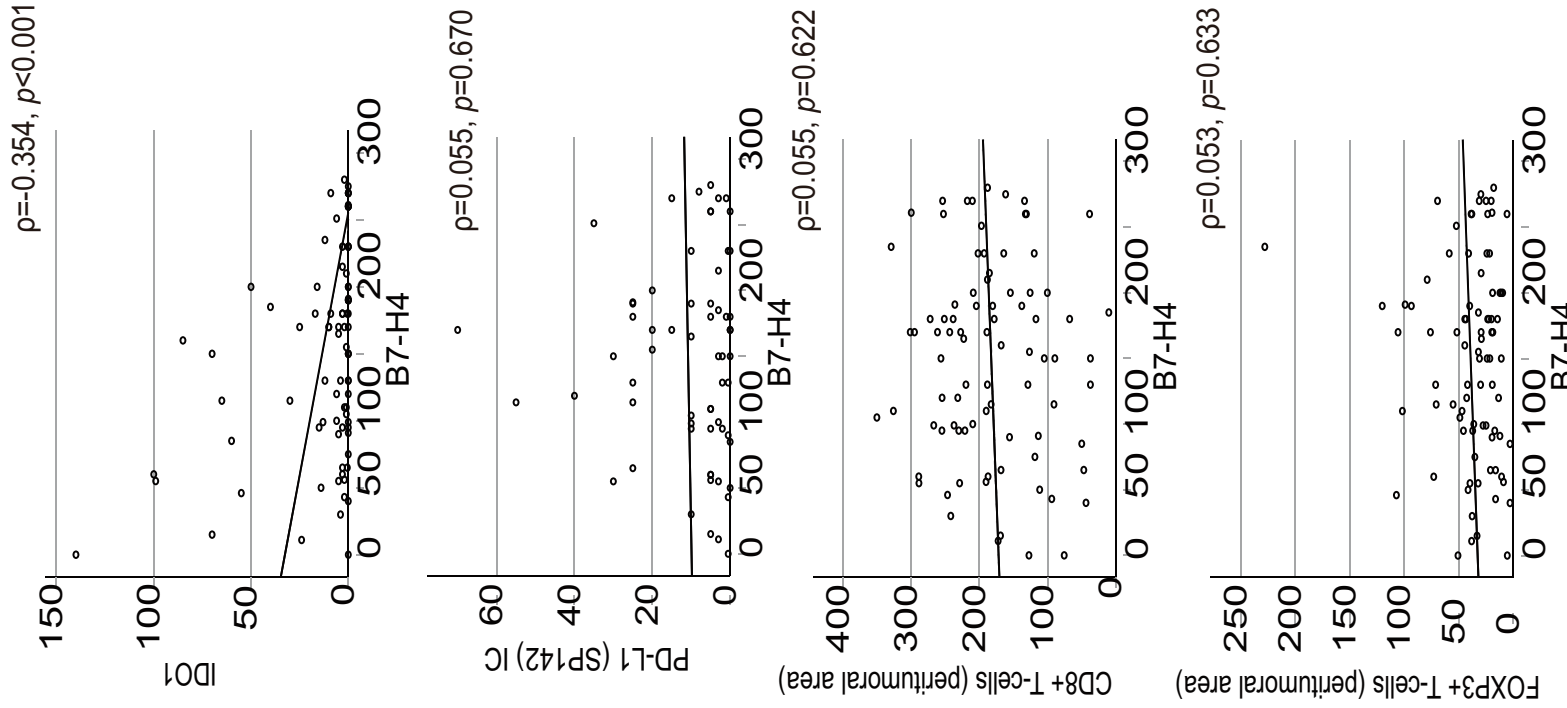




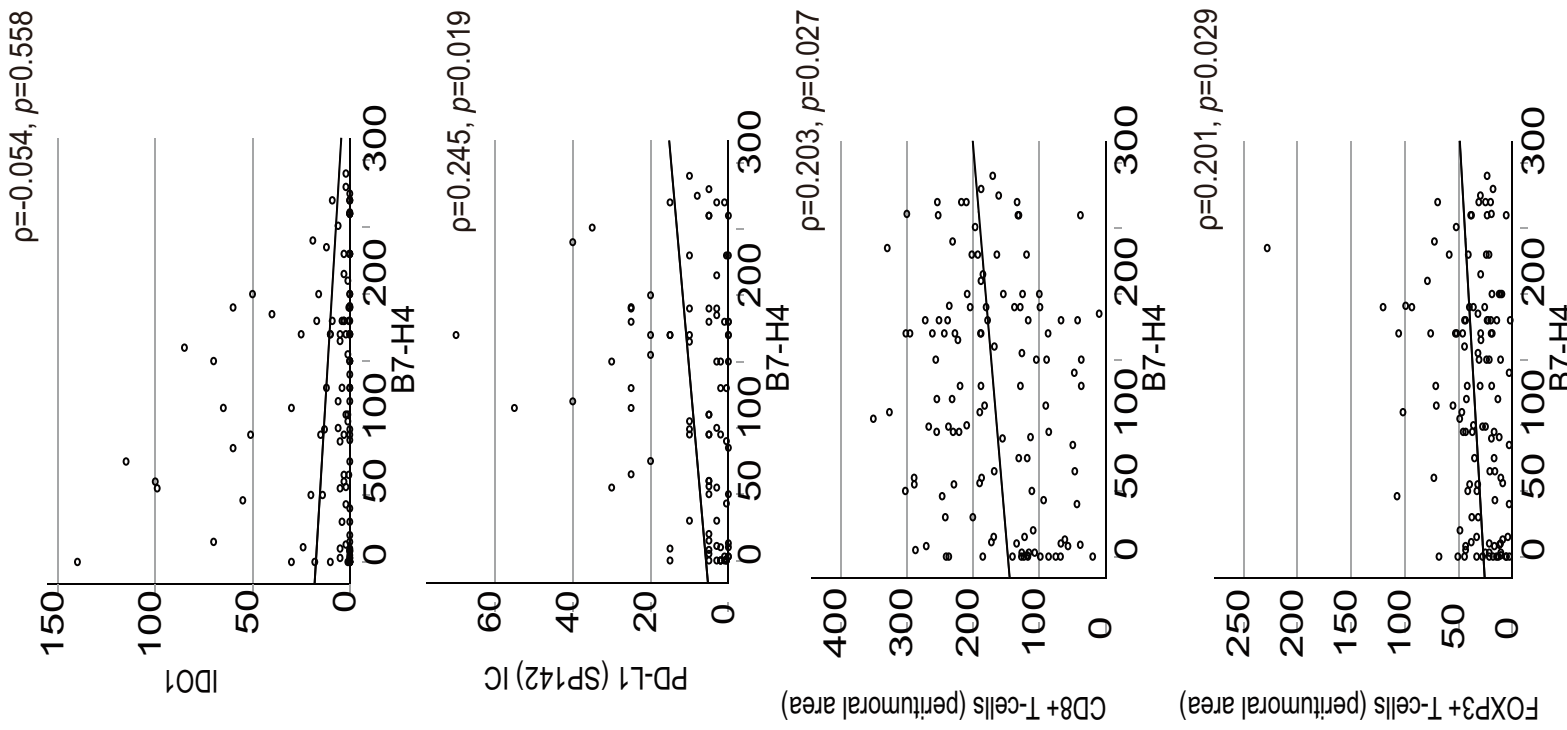




b



a



TABLES

Table 1. Relationship between clinical pathology data and immune checkpoint molecule expression

Variables		B7-H4		<i>p</i> =	IDO1		<i>p</i> =	PD-L1 (28-8)		<i>p</i> =	PD-L1 (SP142)			<i>p</i> =
		n (%)	H-Score ≥120		H-Score ≥1	<1		CPS ≥1	<1		N	≥1	IC <1	
Number of patients	119 (100)	n			n			N			n			
Age (years)				0.0396			0.611			0.134				0.658
	<55	44 (37.0)	28	16	25	19		22	22		32	26	6	
	≥55	75 (63.0)	33	42	39	36		27	48		59	45	14	
Tumor size (cm)				0.288			0.408			0.002				0.137
	<2	70 (58.8)	38	32	38	32		22	48		50	35	15	
	2≤<5	42 (35.3)	18	24	24	18		26	16		35	31	4	
	≥5	7 (5.9)	5	2	2	5		1	6		6	5	1	
Histological grade				0.023			0.714			0.002				0.003
	Low	30 (25.2)	10	20	17	13		5	25		25	14	11	
	High	89 (74.8)	51	38	47	42		44	45		66	57	9	
pV				0.044			0.759			0.316				0.428
	0	86 (72.3)	49	37	47	39		33	53		64	48	16	
	≥1	33 (27.7)	12	21	17	16		16	17		27	23	4	
pLy				0.602			0.945			0.929				0.002
	0	71 (59.7)	35	36	38	33		29	42		49	33	16	
	≥1	48 (40.3)	26	22	26	22		20	28		42	38	4	
pN				0.705			0.2			0.516				0.109
	0	84 (70.6)	44	40	42	42		33	51		61	45	16	
	≥1	35 (29.4)	17	18	22	13		16	19		30	26	4	
Ki-67 labeling index				0.00115			0.611			0.0183				0.139
	<40	44 (37.0)	14	30	25	19		12	32		37	26	11	
	≥40	75 (63.0)	47	28	39	36		37	38		54	45	9	

Stage					1			0.121			0.01			0.022
	I	57 (47.9)	29	28		29	28		16	41		40	26	14
	II	43 (36.1)	22	21		27	16		25	18		36	31	5
	III	17 (14.3)	9	8		6	11		8	9		13	13	0
	IV	2 (1.7)	1	1		2	0		0	2		2	1	1
Histopathologic type					0.008			0.426			0.786			0.01
	IDC (NST)	103 (86.6)	56	47		57	46		45	58		76	64	12
	ILC	1 (0.8)	1	0		1	0		0	1		1	0	1
	ACC	3 (2.5)	2	1		2	1		1	2		3	1	2
	MC	4 (3.4)	2	2		2	2		1	3		4	3	1
	AC	8 (6.7)	0	8		2	6		2	6		7	3	4
AR					<0.001			0.052			0.071			0.592
	<10	84 (70.6)	53	31		50	34		39	45		62	49	13
	≥10	35 (29.4)	8	27		14	21		10	25		29	22	7
CK 5/6					0.019			0.89			0.65			0.884
	<1	49 (42.2)	24	25		25	24		18	31		37	31	6
	1≤<10	26 (22.4)	8	18		14	12		11	15		19	14	5
	≥10	41 (35.3)	27	14		23	18		19	22		32	25	7
Distant recurrence					0.843			0.071			0.31			0.847
	Yes	13 (10.9)	7	6		4	9		4	9		9	7	2
	No	106 (89.1)	54	52		60	46		45	61		82	64	18

Abbreviations: ICM, pV, pathological venous infiltration; pLy, pathological lymphocytic infiltration; pN, pathological lymph node status; IDC (NST), invasive ductal carcinoma (no special type); ILC, invasive lobular carcinoma; ACC, adenoid cystic carcinoma; MC, metaplastic carcinoma; AC, apocrine carcinoma; AR, androgen receptor; CK5/6, cytokeratin 5/6; IDO1, indoleamine 2,3-dioxygenase; PD-L1, programmed death ligand 1; CPS, combined positive score; IC, tumor-infiltrating immune cells.

Table 2. Tumor immune environment correlates with immune checkpoint molecule expression

Variables	B7-H4				IDO1				PD-L1(28-8)				PD-L1(SP142)			
	H-Score		<i>p</i> =		H-Score		<i>p</i> =		CPS		<i>p</i> =		IC		<i>p</i> =	
	n (%)	≥120			≥1	<1			≥1	<1			n	≥1	<1	
Number of patients	119 (100)	N			n				n				n			
sTILs (%)							0.606					0.123				<0.001
<20	51 (42.9)	24	27		22	29			9	42			36	18	18	
≤20 <40	28 (23.5)	14	14		18	10			14	14			24	22	2	
≥40	40 (33.6)	23	17		24	16			26	14			31	31	0	
Pattern of TILs							0.122					0.035				<0.001
Desert	52 (43.7)	23	29		21	31			7	45			37	19	18	
Excluded	32 (26.9)	15	17		21	11			17	15			25	23	2	
Inflamed	35 (29.4)	23	12		22	13			25	10			29	29	0	
CD8+T-cells (T)							0.411					0.524				<0.001
Low (<66)	59 (49.6)	28	31		30	29			16	43			47	29	18	
High (≥66)	60 (50.4)	33	27		34	26			33	27			44	42	2	
CD8+T-cells (P)							0.12					0.082				<0.001
Low (<170)	59 (49.6)	25	34		27	32			16	43			44	27	17	
High (≥170)	60 (50.4)	35	25		37	23			33	27			47	44	3	
FOXP3+T-cells (T)							0.642					0.943				<0.001
Low (<16)	58 (48.7)	31	27		31	27			12	46			42	25	17	
High (≥16)	61 (51.3)	30	31		33	28			37	24			49	46	3	
FOXP3+T-cells (P)							0.316					0.056				<0.001
Low (<29)	58 (48.7)	27	31		26	32			14	44			40	24	16	

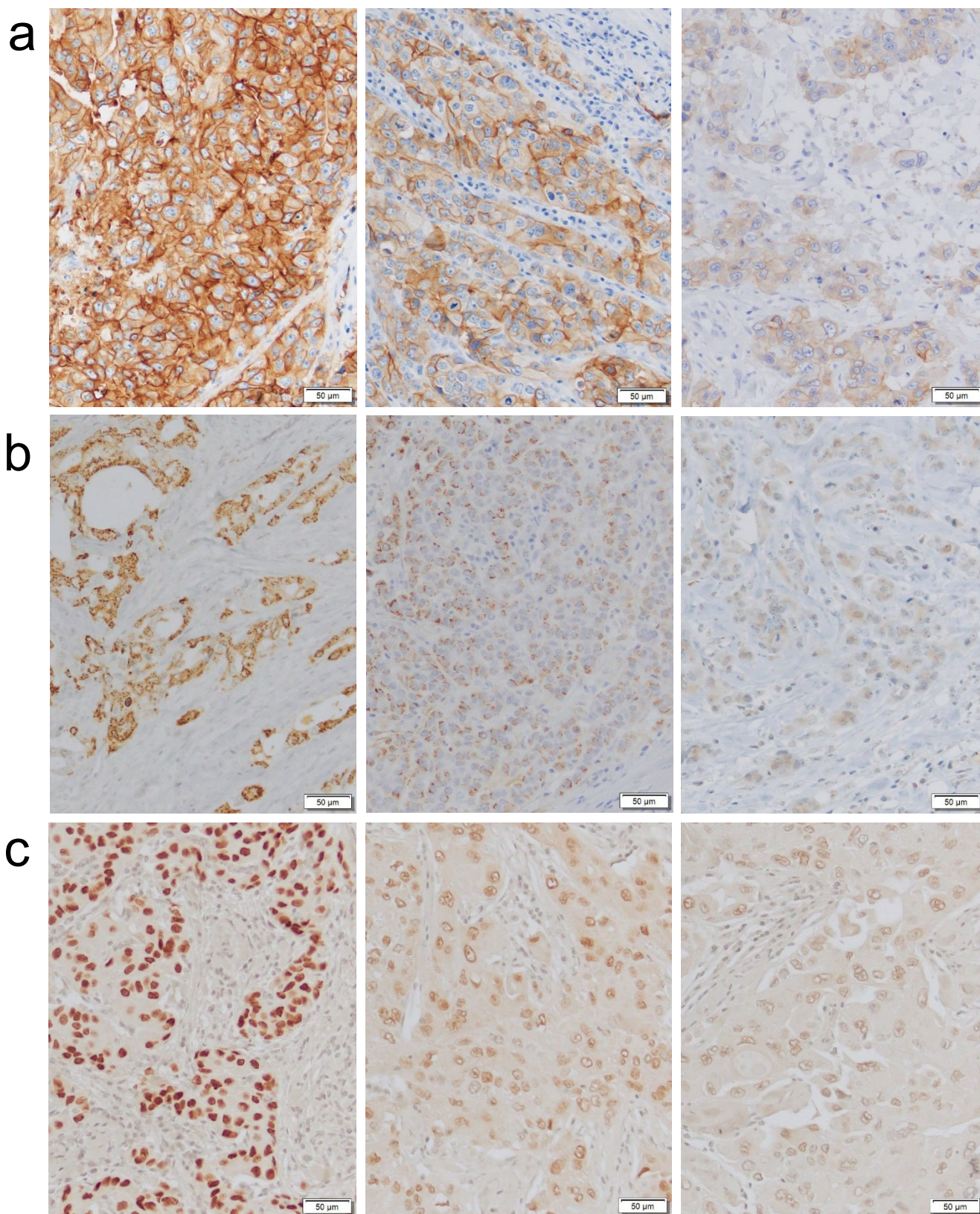


Fig. S1 Representative images of three staining levels (Strong, moderate, and weak) used to determine H-score. a Image of three staining levels of immunostaining for B7-H4. b Image of three staining levels of immunostaining for IDO1. c Image of three staining levels of immunostaining for androgen receptor (AR)

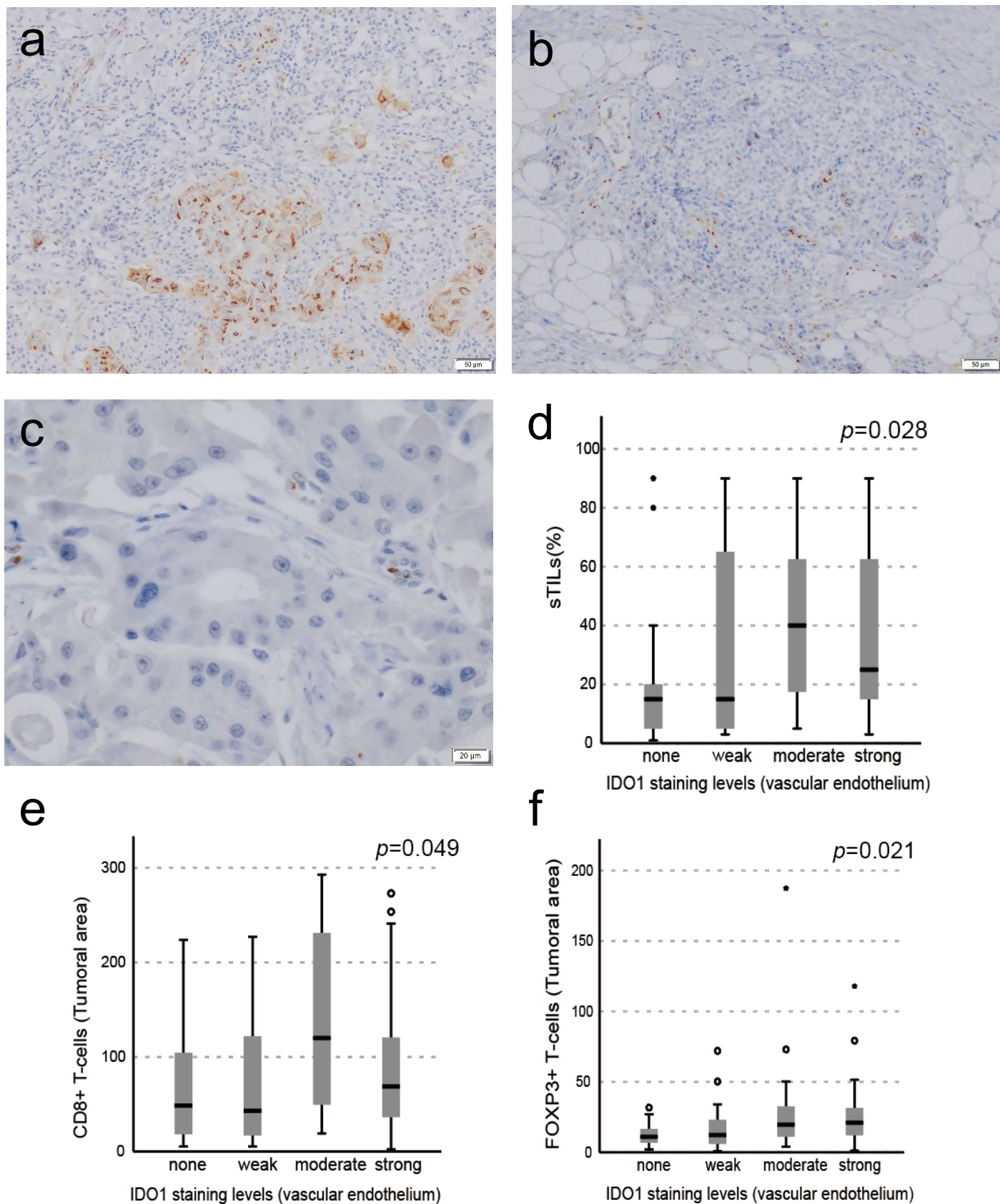


Fig. S2 IDO1 staining of the vascular endothelium and TIME analysis. a image of IDO1-positive tumor and vascular endothelium. b IDO1-positive vascular endothelium in TLS. c IDO1-negative tumor and IDO1-positive vascular endothelium. d analysis of IDO1 staining levels of the vascular endothelium in sTILs (%). e analysis of IDO1 staining levels of the vascular endothelium in CD8+ T-cells (tumoral area). f analysis of IDO1 staining levels of vascular the endothelium in FOXP3+ T-cells

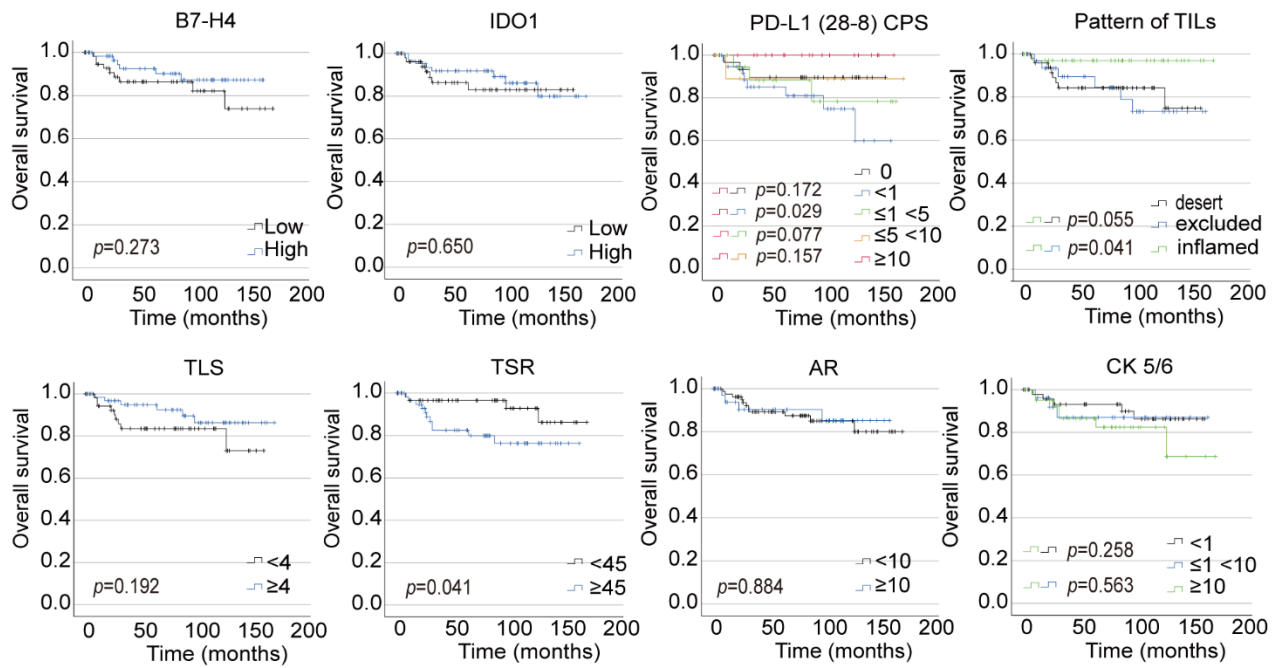


Figure. S3 Overall survival (OS) according to ICM, tumor immune microenvironment (TIME), and triple-negative breast cancer (TNBC) subtypes. Comparison of OS according to B7-H4, IDO1, and PD-L1 levels; TIL pattern; and TLS, TSR, AR, and CK5/6 levels.

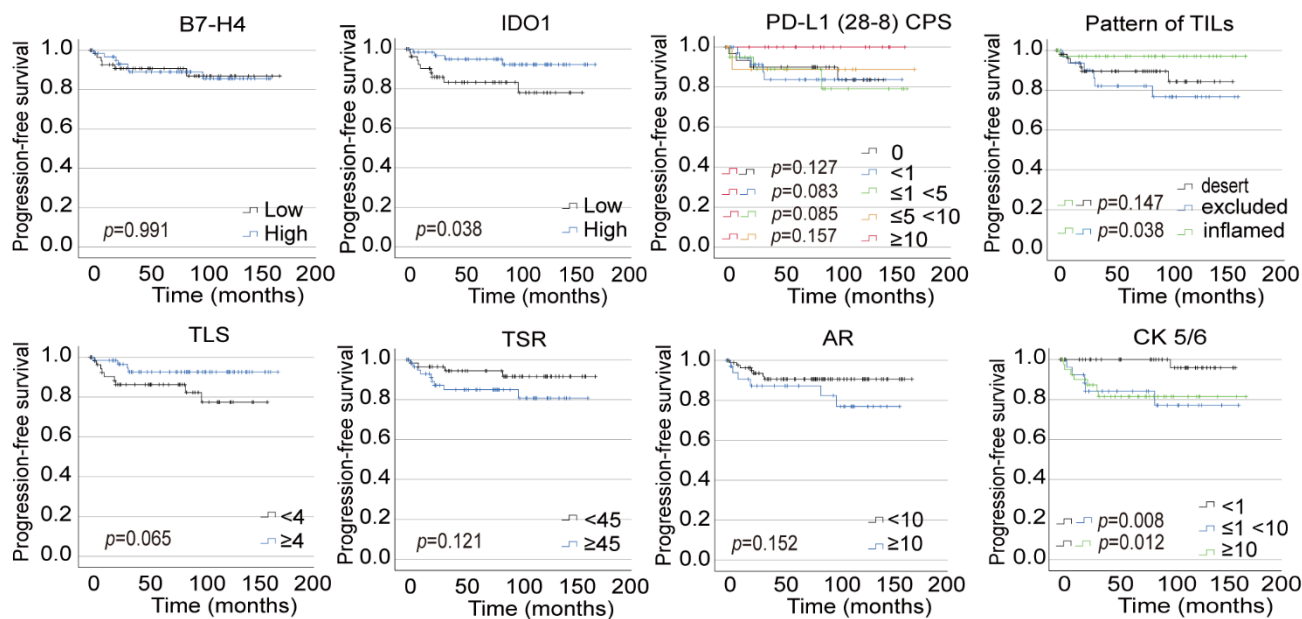


Figure. S4 Progression-free survival (PFS) according to ICM, tumor immune microenvironment (TIME), and triple-negative breast cancer (TNBC) subtypes. Comparison of PFS based on B7-H4, IDO1, and PD-L1 expression

Supplemental Table 1. Staining conditions for the primary antibodies.

Primary antibody	Clone	Vendor (catalog #)	Retrieval	Concentration	Incubation	Linker	Positive control
B7-H4	D1M8I	Cell Signaling (#14572)	Tris-EDTA (pH 9.0), water bath 40 min	1:50	room temp, 30 min		skin (hair follicle)
IDO1	10.1	Merck Millipore (MAB5412)	Tris-EDTA (pH 9.0), pressure cooker, microwave 18 min	1:200	room temp, 30 min		placenta
PD-L1	28-8	Abcam (ab205921)	Universal HIER antigen retrieval reagent (10x) (Abcam). Water bath 40 min	1:400	room temp, 60 min	Envision FLEX+ Rabbit linker, RTU, (Dako), 10 min	tonsil
PD-L1	SP142	Roche (741-4860)	Stained according to fixed protocols for PD-L1 (SP142) on a VENTANA BenchMark ULTRA using Ventana Optiview DAB universal kit and sensitizer.				tonsil
AR	AR441	Agilent (M3562)	Tris-EDTA (pH 9.0), water bath 40 min	1:50	room temp, 30 min		prostate
CK 5/6	D5/16	Dako (GA780)	Tris-EDTA (pH 9.0), water bath 40 min	RTU	room temp, 30 min		tonsil
CD8	SP16	Thermo Fisher (MA5-14548)	Tris-EDTA (pH 9.0), water bath 40 min	1:50	4°C, Over night		tonsil
FOXP3	236A/EA	Abcam (ab20034)	Tris-EDTA (pH 9.0), water bath 20 min	1:100	4 °C, Over night		tonsil

Abbreviations: PD-L1, programmed death-ligand 1; AR, androgen receptor; CK 5/6, cytokeratin 5/6; FOXP3; forkhead box protein P3; EDTA, ethylene diamine tetra acetic acid; HIER, heat-induced epitope retrieval; RTU, ready-to-use.